Estimation of Cooling Circuits' Temperature in Battery Electric Vehicles Using Karhunen Loeve Expansion and LSTM

Marc Sebastián Padrós
Electric Drive Systems
BMW GROUP
Munich, Germany
marc.sebastian-padros@bmw.de

Pascal A. Schirmer
Power Electronics/CIS Group
BMW GROUP/University of Hertfordshire
Munich, Germany
p.schirmer@herts.ac.uk

Iosif Mporas
CIS Group
University of Hertfordshire
Hatfield, UK
i.mporas@herts.ac.uk

***Abstract*—Estimation of vehicle components' temperatures is essential to compute their thermal fatigue and life expectancy, and is typically based on lumped-parameter models, such as thermal networks. However, the design of such models requires expert knowledge and detailed information about the cooling circuit, thus data-driven approaches have been employed. In this article, a regression architecture for estimating the coolant temperature is proposed. The architecture utilizes a two branch LSTM regression model with optimized parameters and is separately modelling active and passive vehicle states. The proposed architecture was evaluated using data from a real battery electric vehicle from 1,000 hours of driving and showed an improvement in performance up-to 36.9% in terms of mean absolute error.**

***Index Terms*—Temperature Estimation, Driving State Indication, Battery Electric Vehicles.**

I. Introduction

Accurate knowledge of component temperatures, e.g. the temperatures of semiconductor or capacitors, is essential to avoid excessive damage and ageing of the components in Battery Electric vehicles (BEVs) [1] and is addressed by thermal modelling twofold. First, thermal modelling is commonly used to estimate temperatures in approximately real time, especially at positions where a sensor cannot be placed effectively, such as close to the rotating parts [2]. Second, thermal models are utilized to estimate the temperatures offline and predict component damages under certain load conditions, thus without online measurements [3].

While high-fidelity thermal models, such as Finite Element Models (FEMs), can estimate temperatures with high accuracy, their computational complexity make them unsuitable for simulations where thousands of different driving scenarios need to be evaluated or when requiring real time capability [4]. Therefore, several reduced-order models have been proposed in the literature [5] , e.g. lumped parameter thermal models, providing a simplified model of the cooling circuit, its geometry and parameters. Furthermore, data-driven models, including State-Space Models (SSMs) [6]–[8] and their variants, e.g. Linear Parameter-Varying SSMs (LPV-SSMs) [9], have been proposed as well.

However, even though SSMs as well as FEMs have proved to work well in terms of estimation accuracy [10], there are two major shortcomings intrinsically related to these approaches. First exhaustive knowledge of the free parameters like the thermal resistances or the geometric parameters is needed [6], [9]. Second, these models suffer from very limited transfer capabilities, thus changes in the architecture of the cooling circuit cannot be easily re-modelled [11]. To overcome these difficulties data-driven regression models have been proposed, with the latest research focusing on LSTM and CNN based architectures [12]–[14], with LSTM showing promising results in terms of estimating the electric motor's stator and rotor temperature due to its ability to model timeseries'. Conversely, errors are relatively high when trying to estimate coolant temperatures [15].

In this paper we propose a LSTM based architecture that is based on two discrete data-driven temperature models, which are separately modelling the active and passive states of a BEV, i.e. the periods where the vehicle is on the move (active) and the charging or standing periods (passive). The remainder of this paper is organized as follows: In Section II the cooling architecture of a BEV is described. In Section III the proposed architecture for temperature estimation is presented. In Sections IV and Section V the experimental setup and the evaluation results are presented, respectively. Conclusions are provided in Section VI.

II. Thermal Management of Electric Vehicles

As described in Section I accurate thermal modelling of BEVs is essential for multiple reasons including lifetime estimation, functional safety and monitoring of the vehicle's status [1]. Especially for the electric components of the vehicle, like the electric motor or the high voltage storage unit, precise estimation of the coolant temperature is crucial due to the high losses and potential failures [16]. The simplified block diagram of the cooling circuit is illustrated in Fig. 1.

As illustrated in Fig. 1 the coolant circuit of a BEV consists of the Highly Integrated Electric Drive Train (HEAT), the Combined Charging Unit (CCU), the High Voltage Storage

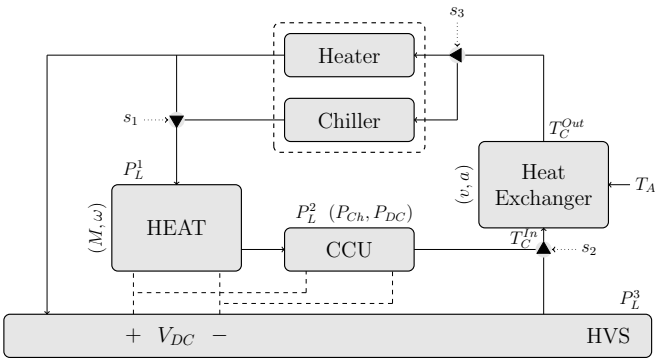

Fig. 1. Illustration of the cooling circuit of a BEV. Solid lines indicate coolant pipes, dashed lines indicated electric connections and dotted lines indicate actuator signals.

(HVS), the Heat Exchanger, the Chiller/Heater and other components (valves and tubing) [17]. The general lumped thermal model of the self-heating and thermal coupling can be described as follows [18], [19]:

$$\begin{bmatrix} T_1 \\ T_2 \\ \vdots \\ T_j \end{bmatrix} = \begin{bmatrix} R_{th}^{11} & R_{th}^{12} & \cdots & R_{th}^{1i} \\ R_{th}^{21} & R_{th}^{22} & \cdots & R_{th}^{2i} \\ \vdots & \vdots & \ddots & \vdots \\ R_{th}^{j1} & R_{th}^{j2} & \cdots & R_{th}^{ji} \end{bmatrix} \cdot \begin{bmatrix} P_{L,1} \\ P_{L,2} \\ \vdots \\ P_{L,j} \end{bmatrix} + \begin{bmatrix} T_{c,1} \\ T_{c,2} \\ \vdots \\ T_{c,j} \end{bmatrix} \quad (1)$$

where T_j, $P_{L,j}$ and $T_{C,j}$ are the temperatures, the losses, and the cooling temperature at the j^{th} node respectively. Furthermore, $R_{th} \in \mathbb{R}^{i \times j}$ is a matrix of thermal resistances describing the steady-state thermal conditions of the cooling circuit.

The coolant temperature is a function of the losses of all components as well as the heat exchange with the environment [10], i.e. $T_C = f(P_L, \dot{Q})$, where $P_L = \sum_j P_{L,j}$ are the total losses and $\dot{Q}$ is the heat flow. Furthermore, the losses depend on the internal driving and charging states, i.e.:

$$P_L = f(M, \omega, V_{DC}, P_{Ch}, P_{DC}) \quad (2)$$

where M is the torque, ω is the rotational speed (driving state), V_{DC} is the voltage of the HVS, P_{Ch} is the charging power (charging state) and P_{DC} is the load of the DCDC converter used by car entertainment loads and lights. Moreover, the heat exchange with the environment strongly depends on the ambient temperature (T_A), the driving condition, i.e. the velocity (v) and acceleration (a) as well as the operation conditions of the chiller/heater and the valves (s).

Modelling all the above-described states and operational conditions is practically impossible [20]. Furthermore, the states heavily rely on whether the vehicle is actively (driving) or passively operating (charging or standing). In addition, the coolant temperature does not only depend on the current state but is also a time-series problem depending on previous states. Therefore, an LSTM based architecture modelling active and passive states is presented in Section III.

III. Proposed Architecture

Considering M sensors acquiring measurements at the same sampling frequency f_s, M time-synchronous frames o_τ^m are formed at time τ with $1 \leq m \leq M$ and o_τ^m, consisting of the last W samples acquired by each sensor $[\tau - W + 1 : \tau]$, i.e. $o_\tau^m \in \mathbb{R}^W$. Each of the M frames o_τ^m is processed by a feature extraction algorithm and M feature vectors, o_τ^D, are generated, one for each frame. The multidimensional feature set $F^\tau \in \mathbb{R}^{M \times D}$, where M is the number of sensors and D is the number of features, is then used to estimate the coolant temperature T_C at time τ, i.e.

$$\hat{T}_C^\tau = r(F^\tau) \quad (3)$$

where $r(\cdot)$ is a regression function modelling the behaviour of the cooling circuit and $\hat{T}_C^\tau$ is the estimated temperature.

As frequency-based features have proved to enhance the estimation accuracy of time-series problems with low sampling frequency [21], [22], and BEV's sensors are usually acquiring data with low sampling frequencies (less than 10 Hz) the Karhunen Loeve Expansion (KLE) has been selected as a frequency domain descriptor [23]–[25]. In detail, let $\widetilde{W}(\widetilde{W} < W)$ be the order of the Auto-Correlation Matrix (ACM) used to separate each time frame o_τ^m into its Subspace Components (SCs). The ACM Φ_{oo} of the τ^{th} frame and of the m^{th} sensor, o_τ^m, can be written as [24]:

$$\Phi_{oo}^{\tau,m} = \begin{bmatrix} R_{oo}^{\tau,m}(0) & \cdots & R_{oo}^{\tau,m}(\widetilde{W}-1) \\ \vdots & \ddots & \vdots \\ R_{oo}^{\tau,m}(\widetilde{W}-1) & \cdots & R_{oo}^{\tau,m}(0) \end{bmatrix} \quad (4)$$

where $R_{oo}^{\tau,m}(w)$ with $0 < w < (\widetilde{W} - 1)$ is the auto-correlation function and w is a positive integer indicating the sample time. By applying eigenvector decomposition, $\Phi_{oo}^{\tau,m}$ can be decomposed into $\widetilde{W}$ mutually orthonormal eigenvectors $Q^{\tau,m} = [q_0^{\tau,m}, q_1^{\tau,m}, \ldots, q_{\widetilde{W}-1}^{\tau,m}]$. Since $Q^{\tau,m}$ is unitary (i.e.,$Q^T Q = QQ^T = I$), the KLE transform and its inverse can be written as in Eq. 5 and Eq. 6.

$$\widetilde{o_\tau}^m = (Q^{\tau,m})^T o_\tau^m \quad (5)$$

$$o_\tau^m = Q^{\tau,m} \widetilde{o_\tau}^m = \sum_{i=0}^{\widetilde{W}-1} (q_i^{\tau,m})^T o_\tau^m q_i^{\tau,m} \quad (6)$$

where, $\widetilde{o}_\tau^m \in \mathbb{R}^{\widetilde{W}}$ denotes the KLE-transformed signal of o_τ^m and the uncorrelated SCs of o_τ^m are defined as $o_i = (q_i^{\tau,m})^T o_\tau^m q_i^{\tau,m}$, where o_i can be approximated by the coefficients of a Finite Impulse Response (FIR) filter [26]. Finally, the M transformed time frames $\widetilde{o}_\tau^m$: $1 \leq m \leq M$ are joined to from a feature matrix, i.e. $F^\tau = [\widetilde{o}_\tau^1, \widetilde{o}_\tau^2, ..., \widetilde{o}_\tau^M]$ with $F^\tau \in \mathbb{R}^{M \times \widetilde{W}}$, while the set of feature matrices F consists of N frames of F^τ, i.e. $F \in \mathbb{R}^{N \times M \times \widetilde{W}}$.

In the proposed architecture the regression function $r(\cdot)$ is using as input a pre-processed version of the original feature

set F providing more detailed information about the driving state, being either active (F_A) or passive (F_P). In detail, a threshold parameter θ defines for how long the vehicle must be inactive, i.e. rotational speed to be $\omega = 0$ for a subsequent number of samples, in order to be categorized as passive, i.e.

$$F_P = \begin{cases} F \ if \ \sum_{\tau_0}^{\tau_0+\theta} 1_{\mathbb{R}>0}(\omega(\tau)) = 0 \\ 0 \ otherwise \end{cases} \quad (7)$$

where τ_0 is an arbitrary starting sample and $1_{\mathbb{R}>0}(\cdot)$ is the indicator function of the rotational speed ω within a time window $[\tau_0 : \tau_0 + \theta]$. The active periods are defined respectively as the inverse of the passive periods, i.e.

$$F_A = \begin{cases} F \ if \ F_P = 0 \\ 0 \ otherwise \end{cases} \quad (8)$$

A feature vector will then be used to generate enhanced prediction based on the temperature model, i.e.

$$\hat{T}_C^\tau = r_C\left(F_A^\tau, F_P^\tau\right) = \begin{cases} r_A(F_A^\tau) \\ r_P(F_P^\tau) \end{cases} \quad (9)$$

where $r_C = [r_A, r_P]$ is a concatenated regression function modelling the behaviour of the cooling circuit during the active and passive states. Furthermore, $F_{A/P}^\tau$ is the τ^{th} frame of the active and passive feature vectors $F_{A/P}$. The block diagram of the proposed architecture is utilizing both active and passive feature vectors and is illustrated in Fig. 2.

As shown in Fig. 2 the architecture consists of five steps, namely the framing of the signal $o^{1,\dots,M}(\tau)$ into time frames $o_\tau^{1,\dots,M}$, the transformation of the time frames into the frequency domain $\tilde{o}_\tau^{1,\dots,M}$, the concatenation of the M sensor signals into one feature set F^τ, the splitting of the driving states separating the feature vector F^τ into its active and passive components F_A^τ and F_P^τ and the estimation of the coolant temperature using the regression function $r_C(\cdot)$.

IV. Experimental Setup

The architecture presented in Section III was evaluated using the datasets, the regression model and experimental protocols described below.

A. Data Structure and Experimental Protocols

To evaluate the proposed architecture two different datasets have been used. First, the publicly available 'Electric Motor Temperature' dataset has been evaluated [14]. This dataset was recorded at a sampling frequency of 2 Hz and a total duration of 185 hrs. It consists of eight features, namely the torque (M), rotational speed (ω), ambient temperature (T_A), cooling temperature (T_C), stator voltages ($u_{d/q}$) and stator currents ($i_{d/q}$). Furthermore, splitting between training and testing data has been defined assuring direct comparison [14]. Second, a reference dataset of a real BMW test vehicle was recorded using the CAN-Bus data at a sampling frequency of 1 Hz and a total duration of approximately 1,000 hrs with a split of 40% active driving phases and 60% passive phases. In detail, the dataset consists of six features, namely the torque (M), rotational speed (ω), current and voltage of the HVS (V_{DC}, I_{DC}), ambient temperature (T_A) and cooling temperature (T_C).

Regarding the experimental setup, two different protocols were used. The first one serves as a baseline system and consists of a single LSTM without distinction of the driving state, similarly to [12]. The second protocol evaluates the architec- ture proposed above based on two LSTM that are applied de- pending on the BEV state. Training/test data splits have been applied as described in [14] for the first dataset, while for the second dataset training and testing was based on five-fold cross validation. Input features have been normalized during pre-processing to [0,1] amplitude range.

B. Regression Model and Parameters Optimization

For the regression stage a LSTM model-based approach same as in [13] was evaluated and tuned using grid search on a bootstrap training dataset optimizing both model structure and free parameters. The model structure is graphically illustrated in Fig. 2, while the parameters of the model as well as the parameters of the Adam solver are tabulated in Table I.

TABLE I
PARAMETERS OF THE LSTM AND THE ADAM SOLVER.

Parameter	Value	Parameter	Value
Input size	64	Learning rate	0.001
Output size	1	Beta-1	0.9
Batch size	1000	Beta-2	0.999
Epochs	200	Epsilon	1e-8

The free parameters θ defining the split between active and passive driving cycles and the frame length W were optimized using grid search. The results in terms of Root Mean Square Error (RMSE) are tabulated in Table II and in Table III.

TABLE II
PARAMETERS OPTIMIZATION (IN TERMS OF RMSE) FOR THE THRESHOLD TIME θ.

θ	60	90	120	150	180
RMSE in (K)	5.82	5.81	6.00	5.86	5.84

TABLE III
PARAMETERS OPTIMIZATION (IN TERMS OF RMSE) FOR THE FRAME LENGTH W.

W	16	32	64	128	256
RMSE in (K)	4.37	3.32	2.38	3.65	6.39

As can be seen in Table II and in Table III, the optimal duration for θ was found to be 90 sec, while the optimal frame length W was found to be 64 samples.

V. Experimental Results

The architecture presented in Section III was evaluated according to the experimental setup described in Section IV. The performance was evaluated in terms of Mean-Absolute-Error (MAE), Mean-Squared-Error (MSE), and RMSE as described in Eq. 10 - Eq. 11.

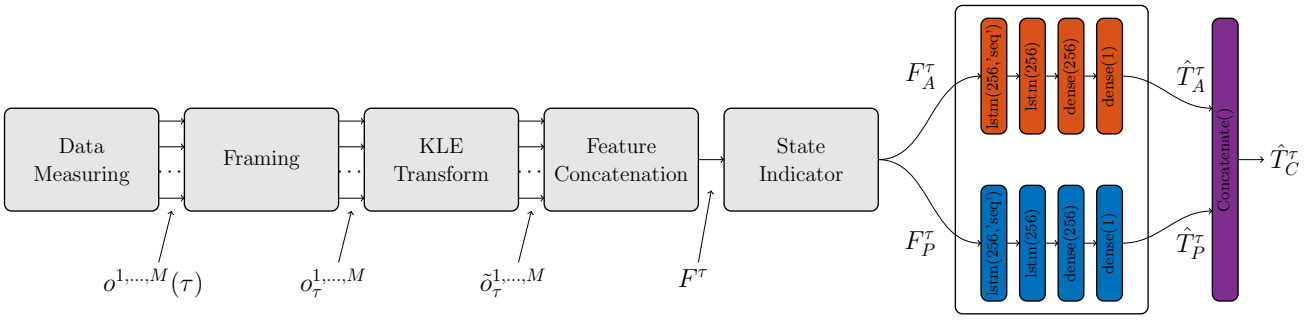

Fig. 2. Block diagram of the proposed architecture for temperature prediction of EVs' coolant circuit temperature.

$$MAE = \frac{1}{N}\sum_{\tau=1}^{N}\left|T_C^\tau - \hat{T}_C^\tau\right| \tag{10}$$

$$RMSE = \sqrt{MSE} = \sqrt{\frac{1}{N}\sum_{\tau=1}^{N}\left(T_C^\tau - \hat{T}_C^\tau\right)^2} \tag{11}$$

where T_C^τ is the ground-truth value of the temperature at time τ and $\hat{T}_C^\tau$ is the predicted value. The two experimental protocols were evaluated for the accuracy metrics described above and the results are tabulated in Table IV. The results for the protocol #2 are presented for the active ('#2-A') and passive ('#2-P') states as well as on average ('#2').

TABLE IV
COOLANT TEMPERATURE ESTIMATION RESULTS FOR THE TWO PROPOSED EXPERIMENTAL PROTOCOLS.

Protocol	Dataset #1		Dataset #2	
	MAE	RMSE	MAE	RMSE
#1	0.55	4.39	5.47	8.01
#2	0.23	2.40	4.06	6.11
#2-A	0.24	3.55	4,26	6,37
#2-P	0.21	0.42	3.45	5.33

As shown in Table IV, the proposed architecture outperforms the baseline model in both datasets and for all performance metrics. Specifically, the passive states showing a higher performance improvement than the active states, which is due to the fact that passive states have a simpler characteristic where many components are not operating. In detail, in dataset #2 the MAE was reduced by 1.41 thus improving temperature prediction by 25.8%, while the RMSE was reduced by 1.90, i.e. improving by 23.7%. Furthermore, the highest performance improvement is found for MAE at the passive phase, reducing the error by 36.9%, while the RMSE was improved by 33.5% . Moreover, the results for dataset #1 are very similar with a lower absolute error due to the lower complexity of the coolant circuit being a test-bench application rather than an actual vehicle as in dataset #2. In general, an performance improvement is observed when incorporating frequency based KLE features and separating active and passive driving states.

As there are few papers estimating coolant temperature, comparison was done using the approaches of [12] and [13] performing stator temperature estimation for four measurement points using the publicly available dataset #1. The results are tabulated in Table V.

TABLE V
COMPARISON OF DIFFERENT ML ARCHITECTURES FOLLOWING THE SETUP OF [12] ESTIMATING STATOR TEMPERATURES.

Model	Approach	MAE	MSE	Mdl Size
KNN	[12]	4.24	26.10	221k
RF	[12]	3.09	16.26	1.1M
SVR	[12]	2.75	13.42	209k
RNN	[13]	1.29	3.26	1.9k
CNN	[13]	0.85	1.52	67k
LSTM	proposed	0.51	1.41	920k

As can be seen in Table V the proposed architecture outperforms all other models reporting MAE equal to 0.51 and MSE equal to 1.41. This corresponds to an improvement of 7.28% in terms of MSE when being compared with [13], while the MAE is being improved by 40% respectively.

VI. CONCLUSION

A two-branch network for modelling the coolant temperature in BEVs using a LSTM for regression was presented. In detail, a data separation stage was proposed to separate the active and passive states of a BEV to train a two-branch model for active and passive states respectively. The proposed architecture significantly improved the performance when directly compared to the baseline system without separated states as well as to the top performing approaches reported in the literature for regression-based BEVs coolant circuit temperature modelling. The proposed architecture was evaluated using two different datasets, i.e. the publicly available 'Electric Motor Temperature' dataset and a second dataset measuring coolant temperatures from real BEVs, reporting performances up-to 0.51 in terms of MAE outperforming all previously reported approaches.

REFERENCES

[1] Frede Blaabjerg, Huai Wang, Ionut Vernica, Bochen Liu, and Pooya Davari, "Reliability of power electronic systems for ev/hev applications," *Proceedings of the IEEE*, vol. 109, no. 6, pp. 1060–1076, 2020.

[2] Christian Kral, Anton Haumer, and Sang Bin Lee, "A practical thermal model for the estimation of permanent magnet and stator winding temperatures," *IEEE Transactions on Power Electronics*, vol. 29, no. 1, pp. 455–464, 2013.

[3] Saeed Peyghami, Tomislav Dragicevic, and Frede Blaabjerg, "Intelligent long-term performance analysis in power electronics systems," *Scientific Reports*, vol. 11, no. 1, pp. 1–18, 2021.

[4] Jimmy Alexander Butron Ccoa, Bastian Strauss, Gerhard Mitic, and Andreas Lindemann, "Investigation of temperature sensitive electrical parameters for power semiconductors (igbt) in real-time applications," in *PCIM Europe 2014; International Exhibition and Conference for Power Electronics, Intelligent Motion, Renewable Energy and Energy Management*. VDE, 2014, pp. 1–9.

[5] Ph Guillemet, Y Scudeller, and Th Brousse, "Multi-level reduced-order thermal modeling of electrochemical capacitors," *Journal of Power Sources*, vol. 157, no. 1, pp. 630–640, 2006.

[6] T Huber, W Peters, and J Bocker, "A low-order thermal model for monitoring critical temperatures in permanent magnet synchronous motors," 2014.

[7] S Kar Chowdhury and Prem Kr Baski, "A simple lumped parameter thermal model for electrical machine of tefc design," in *2010 Joint International Conference on Power Electronics, Drives and Energy Systems & 2010 Power India*. IEEE, 2010, pp. 1–7.

[8] PH Mellor, D Roberts, and DR Turner, "Lumped parameter thermal model for electrical machines of tefc design," in *IEE Proceedings B (Electric Power Applications)*. IET, 1991, vol. 138, pp. 205–218.

[9] Fang Qi, Duy An Ly, Christoph van der Broeck, Decheng Yan, and Rik W De Doncker, "Model order reduction suitable for online linear parameter-varying thermal models of electric motors," in *2016 IEEE 2nd Annual Southern Power Electronics Conference (SPEC)*. IEEE, 2016, pp. 1–6.

[10] Amir Sajjad Bahman, Ke Ma, and Frede Blaabjerg, "Thermal impedance model of high power igbt modules considering heat coupling effects," in *2014 International Power Electronics and Application Conference and Exposition*. IEEE, 2014, pp. 1382–1387.

[11] Ze Wang and Wei Qiao, "A physics-based improved cauer-type thermal equivalent circuit for igbt modules," *IEEE Transactions on Power Electronics*, vol. 31, no. 10, pp. 6781–6786, 2016.

[12] Wilhelm Kirchgässner, Oliver Wallscheid, and Joachim Böcker, "Data-driven permanent magnet temperature estimation in synchronous motors with supervised machine learning: A benchmark," *IEEE Transactions on Energy Conversion*, 2021.

[13] Wilhelm Kirchgässner, Oliver Wallscheid, and Joachim Böcker, "Deep residual convolutional and recurrent neural networks for temperature estimation in permanent magnet synchronous motors," in *2019 IEEE International Electric Machines & Drives Conference (IEMDC)*. IEEE, 2019, pp. 1439–1446.

[14] Wilhelm Kirchgässner, Oliver Wallscheid, and Joachim Böcker, "Estimating electric motor temperatures with deep residual machine learning," *IEEE Transactions on Power Electronics*, vol. 36, no. 7, pp. 7480–7488, 2020.

[15] Rajeshwar Yadav, "Modeling and analysis of energy consumption in chevrolet volt gen ii hybrid electric vehicle," 2018.

[16] Sajib Chakraborty, Mohammed Mahedi Hasan, Paul McGahan, Thomas Geury, Pooya Davari, Frede Blaabjerg, Mohamed El Baghdadi, Omar Hegazy, et al., "Real-life mission profile oriented lifetime estimation of a sic interleaved bidirectional hv dc/dc converter for electric vehicle drivetrains," *IEEE Journal of Emerging and Selected Topics in Power Electronics*, 2022.

[17] Jaewan Kim, Jinwoo Oh, and Hoseong Lee, "Review on battery thermal management system for electric vehicles," *Applied thermal engineering*, vol. 149, pp. 192–212, 2019.

[18] Mengxing Chen, Huai Wang, Donghua Pan, Xiongfei Wang, and Frede Blaabjerg, "Thermal characterization of silicon carbide mosfet module suitable for high-temperature computationally efficient thermal-profile prediction," *IEEE Journal of Emerging and Selected Topics in Power Electronics*, vol. 9, no. 4, pp. 3947–3958, 2020.

[19] Haoran Wang and Huai Wang, "An analytical circuit based nonlinear thermal model for capacitor banks," *Microelectronics reliability*, vol. 88, pp. 524–527, 2018.

[20] Xiping Wang, Zhigang Li, Fang Yao, and Shengxue Tang, "Simplified estimation of junction temperature fluctuation at the fundamental frequency for igbt modules considering mission profile," *IEEE Access*, vol. 7, pp. 149308–149317, 2019.

[21] Pascal A Schirmer and Iosif Mporas, "Energy disaggregation from low sampling frequency measurements using multi-layer zero crossing rate," in *ICASSP 2020-2020 IEEE International Conference on Acoustics, Speech and Signal Processing (ICASSP)*. IEEE, 2020, pp. 3777–3781.

[22] Pascal A Schirmer and Iosif Mporas, "Low-frequency energy disaggregation based on active and reactive power signatures," in *2021 29th European Signal Processing Conference (EUSIPCO)*. IEEE, 2021, pp. 1426–1430.

[23] Shirantha Welikala, Chinthaka Dinesh, Mervyn Parakrama B Ekanayake, Roshan Indika Godaliyadda, and Janaka Ekanayake, "Incorporating appliance usage patterns for non-intrusive load monitoring and load forecasting," *IEEE Transactions on Smart Grid*, vol. 10, no. 1, pp. 448–461, 2017.

[24] Chinthaka Dinesh, Buddhika W Nettasinghe, Roshan Indika Godaliyadda, Mervyn Parakrama B Ekanayake, Janaka Ekanayake, and Janaka V Wijayakulasooriya, "Residential appliance identification based on spectral information of low frequency smart meter measurements," *IEEE Transactions on smart grid*, vol. 7, no. 6, pp. 2781–2792, 2015.

[25] Shirantha Welikala, Chinthaka Dinesh, Roshan Indika Godaliyadda, Mervyn Parakrama B Ekanayake, and Janaka Ekanayake, "Robust non-intrusive load monitoring (nilm) with unknown loads," in *2016 IEEE international conference on information and automation for sustainability (ICIAfS)*. IEEE, 2016, pp. 1–6.

[26] HGCP Dinesh, DBW Nettasinghe, GMRI Godaliyadda, MPB Ekanayake, JV Wijayakulasooriya, and JB Ekanayake, "A subspace signature based approach for residential appliances identification using less informative and low resolution smart meter data," in *2014 9th International conference on industrial and information systems (ICIIS)*. IEEE, 2014, pp. 1–6.